

## Time-independent measurements of the CKM angle $\gamma$

---

**Sneha Malde<sup>a,\*</sup> on behalf of the LHCb Collaboration**

<sup>a</sup>University of Oxford,

Keble Rd, Oxford, United Kingdom

E-mail: [sneha.malde@physics.ox.ac.uk](mailto:sneha.malde@physics.ox.ac.uk)

A goal of the LHCb experiment is to measure the CKM angle with a precision of  $1^\circ$ . At this precision it is hoped that hints or indeed an observation of physics beyond the standard model could arise. In order to reach this precision it will be necessary to target a number of decays modes. Results from two analyses are presented here which make use of the entire Run1 and Run2 dataset collected at the LHCb experiment. One of them leads to a measurement of  $\gamma = (68.7_{-5.2}^{+5.2})^\circ$ , which is the most precise result from a single measurement.

*40th International Conference on High Energy physics - ICHEP2020  
July 28 - August 6, 2020  
Prague, Czech Republic (virtual meeting)*

---

\*Speaker

## 1. Introduction

A precise measurement of the CKM angle  $\gamma$  is highly desirable. Assuming the absence of new physics within tree-level decays, the direct measurement of  $\gamma$  forms a Standard Model benchmark. Through the use of other CKM observables an indirect determination of  $\gamma$  can be made which is driven by the measurement of the angle  $\beta$  and the ratio of  $\Delta(m_s)/\Delta(m_d)$ , both of which are loop-level processes and hence their values could be altered by new physics particles participating within the virtual loops [1]. The CKMfitter group determines that the combination of all direct measurements of  $\gamma = (72.1_{-5.7}^{+5.4})^\circ$ , while an indirect determination that excludes the direct measurements leads to  $\gamma = (65.66_{-2.65}^{+0.90})^\circ$  [2]. It is clear that a reduction in the uncertainty associated with the direct measurements is required to enable the chance to observe a discrepancy between these two values of  $\gamma$ . The measurements presented here are performed with all available data from Run1 and Run2 of the LHCb experiment.

## 2. Measurement of $\gamma$ in $B^\pm \rightarrow Dh^\pm$ , $D \rightarrow K_S^0\pi^+\pi^-$ and $D \rightarrow K_S^0K^+K^-$

The full details of this analysis can be found in Ref [3]. The CKM angle  $\gamma$  can be measured in decays such as  $B^\pm \rightarrow DK^\pm$  where the  $D$  meson decays to a final state that is accessible to both the  $D^0$  and  $\bar{D}^0$  mesons. This leads to interference between the two possible decay modes. Where the  $D$  decays to a self-conjugate final state that has  $CP$ -even fraction close to 0.5, as is the case for  $D \rightarrow K_S^0\pi^+\pi^-$  and  $D \rightarrow K_S^0K^+K^-$  decays, the sensitivity to  $\gamma$  comes from the differences in the  $D$ -meson Dalitz plot distribution between  $B^+$  and  $B^-$  decays [4]. The  $D$ -decay Dalitz plot, based on axes of  $m_+^2$  and  $m_-^2$ , which are the invariant masses of the  $K_S^0$  meson and  $\pi^+$  or  $\pi^-$  meson, respectively, is partitioned into  $2\mathcal{N}$  regions labelled from  $i = -\mathcal{N}$  to  $i = +\mathcal{N}$  (excluding zero), symmetric around  $m_-^2 = m_+^2$  such that if  $(m_-^2, m_+^2)$  is in bin  $i$  then  $(m_+^2, m_-^2)$  is in bin  $-i$ . The bins for which  $m_-^2 > m_+^2$  are defined to have positive values of  $i$ . The value of  $\mathcal{N}$  is 8 for  $D \rightarrow K_S^0\pi^+\pi^-$  decays and 2 for  $D \rightarrow K_S^0K^+K^-$  decays. The parameters  $F_i$  are defined as the fraction of  $D^0$  mesons decaying into bin  $i$  of the Dalitz plot, taking into account the reconstruction and trigger efficiencies of the LHCb detector and the analysis selection requirement. The  $B^+$  or  $B^-$  yield in each bin is then given by

$$\begin{aligned}
 N_{+i}^+ &= h_{B^+} \left[ F_{-i} + \left( (x_+^{DK})^2 + (y_+^{DK})^2 \right) F_{+i} + 2\sqrt{F_i F_{-i}} \left( x_+^{DK} c_{+i} - y_+^{DK} s_{+i} \right) \right], \\
 N_{-i}^+ &= h_{B^+} \left[ F_{+i} + \left( (x_+^{DK})^2 + (y_+^{DK})^2 \right) F_{-i} + 2\sqrt{F_i F_{-i}} \left( x_+^{DK} c_{+i} + y_+^{DK} s_{+i} \right) \right], \\
 N_{+i}^- &= h_{B^-} \left[ F_{+i} + \left( (x_-^{DK})^2 + (y_-^{DK})^2 \right) F_{-i} + 2\sqrt{F_i F_{-i}} \left( x_-^{DK} c_{+i} + y_-^{DK} s_{+i} \right) \right], \\
 N_{-i}^- &= h_{B^-} \left[ F_{-i} + \left( (x_-^{DK})^2 + (y_-^{DK})^2 \right) F_{+i} + 2\sqrt{F_i F_{-i}} \left( x_-^{DK} c_{+i} - y_-^{DK} s_{+i} \right) \right],
 \end{aligned} \tag{1}$$

where  $h$  are normalisation constants, and the sensitivity to  $\gamma$  comes from the cartesian parameters  $x_\pm^{DK} \equiv r_B^{DK} \cos(\delta_B^{DK} \pm \gamma)$  and  $y_\pm^{DK} \equiv r_B^{DK} \sin(\delta_B^{DK} \pm \gamma)$ . Hence the ratio between the suppressed and favoured  $B$ -meson decay,  $r_B^{DK}$  and the strong-phase difference between the two decays,  $\delta_B^{DK}$  are also determined in this analysis. The parameters  $c_i$  ( $s_i$ ) are the cosine (sine) of the amplitude

weighted strong-phase difference of the neutral  $D$  mesons, averaged over the Dalitz plot region. These parameters can be measured through the decay of the  $\psi(3770)$  decay to two neutral  $D$  mesons. Such measurements were first performed by the CLEO collaboration [5] and more recently, with a larger dataset by the BESIII collaboration. The combination of the results are presented in [6, 7], and are used in this analysis. The use of these parameters is crucial since it allows results of this analysis to be independent of any amplitude model of the  $D^0$  decay.

In order to determine the  $F_i$  parameters, the  $B^\pm \rightarrow D\pi^\pm$  decay is considered simultaneously, since the variation in the relative efficiency on the Dalitz plot is the same as that for  $B^\pm \rightarrow DK^\pm$ . The  $B^\pm \rightarrow D\pi^\pm$  decay has weak sensitivity to  $\gamma$  since the value of  $r_B$  in this decay mode is about 20 times smaller than that in  $B^\pm \rightarrow DK^\pm$ . Nonetheless the  $CP$  violation in this decay mode is parameterised by using equations analogous to Eq. 1. One slight difference is that since the value of  $r_B^{D\pi}$  is small, the fit is not stable for a simultaneous fit of the cartesian parameters for both decay modes. Instead use is made of the fact that  $\gamma$  is common to both decay modes and the cartesian parameters for the  $B^\pm \rightarrow D\pi^\pm$  decay mode are parameterised by two parameters  $x_\xi^{D\pi}$  and  $y_\xi^{D\pi}$  such that  $x_\pm^{D\pi} = x_\xi^{D\pi} x_\pm^{DK} - y_\xi^{D\pi} y_\pm^{DK}$  and  $y_\pm^{D\pi} = x_\xi^{D\pi} y_\pm^{DK} + y_\xi^{D\pi} x_\pm^{DK}$ .

The invariant-mass distribution of the selected data is fit to determine the various signal and background contributions. The projections of this fit are shown for  $D \rightarrow K_S^0 \pi^+ \pi^-$  candidates in Fig. 1. The fit is performed separately for  $K_S^0$  candidate mesons that decay early and leave hits in the VELO sub-detector, denoted *long*, and those that decay further downstream, denoted *downstream*, since this leads to slightly different resolutions and background contamination. The results of this fit are used to determine the signal and background parameterisations used in a subsequent fit. The  $B^\pm \rightarrow DK^\pm$  signal yields are approximately 13600 (1900) in the  $D \rightarrow K_S^0 \pi^+ \pi^-$  ( $D \rightarrow K_S^0 K^+ K^-$ ) decay modes. In the subsequent fit, the data are divided into their Dalitz plot regions and a simultaneous fit performed to the invariant-mass distributions in each region to determine the  $CP$  observables. The Dalitz plots of candidates in the signal region are shown in Fig. 2, where indeed it is possible to see the effects of  $CP$  violation by noticeable differences between the two plots.

The systematic uncertainties are very small compared to the statistical uncertainties, and substantially smaller than previous measurements of this decay with smaller data sets. This is because the improved precision of the charm strong-phase parameters leads to an associated uncertainty on  $\gamma$  of less than a degree. The use of the  $B^\pm \rightarrow D\pi^\pm$  mode to determine the efficiency removes the largest LHCb-related uncertainty in comparison to the previous result. Other uncertainties relating to mass models and background parameterisations remain small. Since the analysis considers only the distribution over the Dalitz plot the results are insensitive to the  $B^\pm$  production asymmetry or the detection asymmetry of the kaon or pion originating from the decay of the  $B^\pm$ .

The measured values for the  $CP$  observables and their uncertainties are then interpreted to determine the best fit values for  $\gamma$  and the hadronic parameters. The interpretation is done via a maximum likelihood fit using a frequentist treatment as described in Ref. [8]. The solution for the physics parameters has a two-fold ambiguity as the equations are invariant under the simultaneous substitutions  $\gamma \rightarrow \gamma + 180^\circ$  and  $\delta_B \rightarrow \delta_B + 180^\circ$ . The solution that satisfies  $0 < \gamma < 180^\circ$  is chosen, and leads to  $\gamma = (68.7^{+5.2}_{-5.1})^\circ$ ,  $r_B^{DK^\pm} = 0.0904^{+0.0077}_{-0.0075}$ ,  $\delta_B^{DK^\pm} = (118.3^{+5.5}_{-5.6})^\circ$ ,  $r_B^{D\pi^\pm} = 0.0050 \pm 0.0017$ ,  $\delta_B^{D\pi^\pm} = (291^{+24}_{-26})^\circ$ . The hadronic parameters of the  $B^\pm \rightarrow DK^\pm$  decay are consistent with current averages, and those of the  $B^\pm \rightarrow D\pi^\pm$  decay are obtained with the best precision to date, and have not previously been measured using these  $D$ -decay modes. The CKM angle  $\gamma$  is the most precise

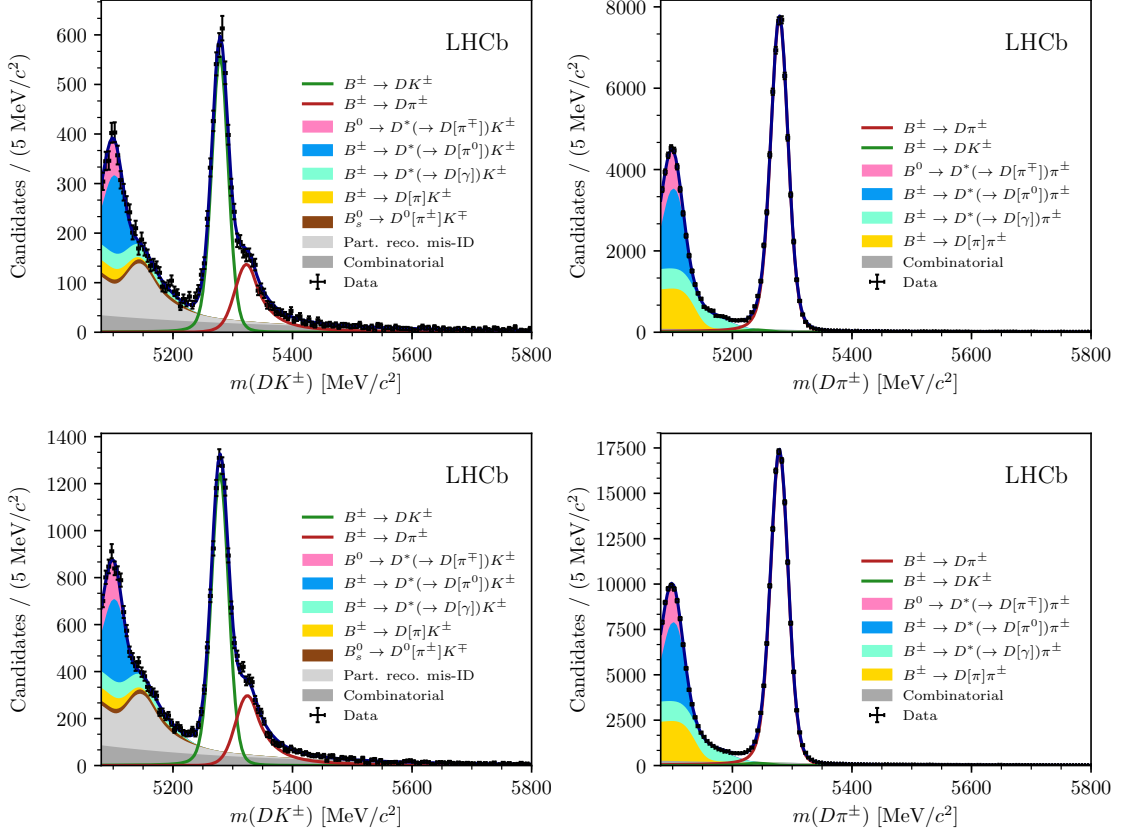


**Figure 1:** Invariant mass distributions for the (left)  $B^+ \rightarrow DK^+$  channel and (right)  $B^+ \rightarrow D\pi^+$  channel with  $D \rightarrow K_S^0\pi^+\pi^-$ . The top (bottom) plots show data where the  $K_S^0$  candidate is long (downstream). A particle within square brackets in the legend denotes the particle that has not been reconstructed.

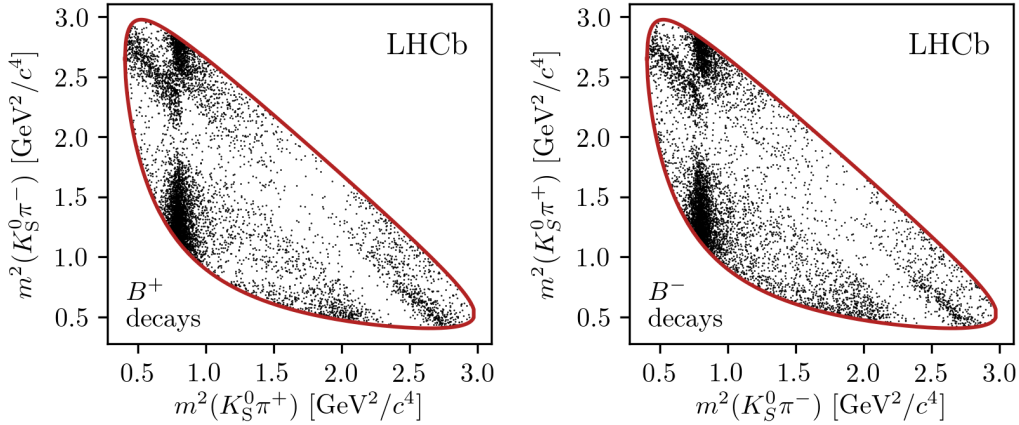


**Figure 2:** Dalitz plot for  $D$  decays of (left)  $B^+ \rightarrow DK^+$  and (right)  $B^- \rightarrow DK^-$  candidates in the signal region, in the  $D \rightarrow K_S^0\pi^+\pi^-$  decay. The horizontal and vertical axes are interchanged between the  $B^+$  and  $B^-$  decay plots to aid visualisation of the  $CP$  asymmetries between the two distributions.

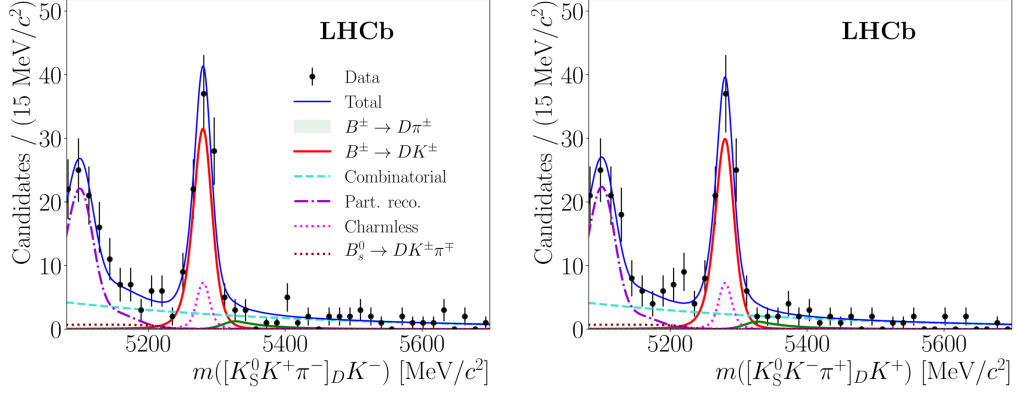


**Figure 3:** Invariant mass of OS  $B^+ \rightarrow DK^+$ ,  $D \rightarrow K_S^0 K^- \pi^+$  (charge conjugate implied) candidates within the  $K^{*\pm}$  region. Candidates containing both long and downstream  $K_S^0$  mesons are shown.

measurement of  $\gamma$  from a single analysis.

### 3. Measurement of $CP$ observables in $B^\pm \rightarrow Dh^\pm$ decays with $D \rightarrow K_S^0 K\pi$

The full details of this analysis can be found in Ref. [9]. The Dalitz plot of the  $D$  decay is split into two regions - one that encompasses the  $K^{*\pm}$  intermediate resonance, and the other the remaining region. The necessary strong-phase parameters have been measured at CLEO [10] for the  $K^{*\pm}$  region and hence the  $CP$  observables from these  $B$  decays can be included in a  $\gamma$  measurement immediately, whereas the observables of the non- $K^{*\pm}$  region can't. Eight yields are considered for each Dalitz plot region. These are the number of  $B^\pm \rightarrow DK^\pm$  or  $B^\pm \rightarrow D\pi^\pm$  signal candidates observed, split by the charge of the decaying  $B$  meson and within each  $B^\pm$  decay the data are further divided into two cases depending on whether the kaon from the  $D$  decay has the same charge (SS) or opposite charge (OS) as the kaon or pion that originates from the  $B$  meson decay. The yield of each category is dependent on  $\gamma$ ,  $r_B$ ,  $\delta_B$  and the strong-phase parameters  $r_D$ ,  $\kappa_D$  and  $\delta_D$  [11], for example

$$N_{OS}^{DK^\pm} \propto r_B^{DK^2} + r_D^2 + 2r_B^{DK} r_D \kappa_D \cos(\delta_B^{DK} \pm \gamma + \delta_D). \quad (2)$$

In practice the yields are combined into asymmetries and ratios to reduce systematic uncertainties and these are the measured  $CP$  observables. An example of the fit to the invariant-mass spectrum is provided in Fig. 3. The low yields mean that  $CP$  violation is not yet observed, and that the measurements are dominated by their statistical uncertainty. Furthermore it is not possible to use these measurements to set direct constraints on  $\gamma$ , rather the  $CP$  observables are used in the combination to improve the overall precision of  $\gamma$ .

## 4. Conclusions

Analyses of the full Run1 and Run2 data from LHCb show striking signs of  $CP$  violation. The analysis of  $B^\pm \rightarrow Dh^\pm$  with  $D \rightarrow K_S^0 h^+ h^-$  leads to a measurement that is of comparable precision to the combination of all other measurements before it. The precision of  $\gamma$  will improve

when these results are combined with those of  $B^\pm \rightarrow Dh^\pm$ ,  $D \rightarrow K_S^0 K\pi$ , and the many other upcoming measurements using other  $D$  and  $B$  decays to measure  $\gamma$ . This improved precision is vital to understand the Standard Model better and potentially uncover the effects of the physics beyond the Standard Model.

## References

- [1] M. Blanke and A. J. Buras, *Universal Unitarity Triangle 2016 and the tension between  $\Delta M_{s,d}$  and  $\epsilon_K$  in CMFV models*, *Eur. Phys. J C* **76** 2016 197, [arXiv:1602.04020]
- [2] [CKMFitter group] J. Charles *et al.*, *Updated results and plots available at: <http://ckmfitter.in2p3.fr>*, *Eur. Phys. J C* **41** 2005 1, [hep-ph/0406184]
- [3] [LHCb Collaboration] R. Aaij *et al.*, *Measurement of the CKM angle  $\gamma$  in  $B^\pm \rightarrow DK^\pm$  and  $B^\pm \rightarrow D\pi^\pm$  decays with  $D \rightarrow K_S h^+ h^-$* , submitted to JHEP, [arXiv:2010.08483]
- [4] A. Giri, Y. Grossman, A. Soffer and J. Zupan, *Determining  $\gamma$  using  $B^\pm \rightarrow DK^\pm$  with multibody  $D$  decays* *Phys.Rev.* **D68** 2003 054018, [hep-ph/0303187], A. Bondar, *Proceedings of BINP special analysis meeting on Dalitz analysis, 24-26 Sep. 2002, unpublished*, [Belle Collaboration] A. Poluektov *et al.*, *Measurement of  $\phi_3$  with Dalitz plot analysis of  $B^+ \rightarrow D^{(*)} K^\pm$  decay*, *Phys.Rev.* **D70** 2004 072003, [hep-ex/0406067]
- [5] [CLEO Collaboration] J. Libby *et al.*, *Model-independent determination of the strong-phase difference between  $D^0$  and  $\bar{D}^0 \rightarrow K_{S,L}^0 h^+ h^-$  ( $h = \pi, K$ ) and its impact on the measurement of the CKM angle  $\gamma/\phi_3$* , *Phys.Rev.* **D82** 2010 112006, [arXiv:1010.2817]
- [6] [BESIII Collaboration] M. Ablikim *et al.*, *Model-independent determination of the relative strong-phase difference between  $D^0$  and  $\bar{D}^0 \rightarrow K_{S,L}^0 \pi^+ \pi^-$  and its impact on the measurement of the CKM angle  $\gamma/\phi_3$* , **D101** 2020 112002, [arXiv:2003.00091]
- [7] [BESIII Collaboration] M. Ablikim *et al.*, *Improved model-independent determination of the strong-phase parameters difference between  $D^0$  and  $\bar{D}^0 \rightarrow K_{S,L}^0 K^+ K^-$* , *Phys.Rev.* **D102** 2020 052008, [arXiv:2007.07959]
- [8] [LHCb Collaboration] R. Aaij *et al.*, *Measurement of the CKM angle  $\gamma$  from a combination of LHCb results*, *JHEP* 12 087 2016, [arXiv:1611.03076]
- [9] [LHCb Collaboration] R. Aaij *et al.*, *Measurement of CP observables in  $B^\pm \rightarrow DK^\pm$  and  $B^\pm \rightarrow D\pi^\pm$  with  $D \rightarrow K_S^0 K^\pm \pi^\mp$  decays*, *JHEP* 06 058 2020, [arXiv:2002.08858]
- [10] [CLEO Collaboration] J. Insler *et al.*, *Studies of the decays  $D^0 \rightarrow K_S^0 K^- \pi^+$  and  $D^0 \rightarrow K_S^0 K^+ \pi^-$* , *Phys.Rev.* **D85** 2012 092016, [arXiv:1203.3804]
- [11] Y. Grossman, Z. Ligeti Zoltan and A. Soffer, *Measuring  $\gamma$  in  $B^\pm \rightarrow K^\pm (KK^*)_D$  decays*, *Phys.Rev.* **D67** 2003 071301, [hep-ph/0210433]